

# 3D Models of MBP, a Biologically Active Metabolite of Bisphenol A, in Human Estrogen Receptor $\alpha$ and Estrogen Receptor $\beta$

Michael E. Baker<sup>1\*</sup>, Charlie Chandsawangbhuwana<sup>2</sup>

<sup>1</sup> Department of Medicine, University of California San Diego, La Jolla, California, United States of America, <sup>2</sup> Department of Bioengineering, University of California San Diego, La Jolla, California, United States of America

## Abstract

Bisphenol A [BPA] is a widely dispersed environmental chemical that is of much concern because the BPA monomer is a weak transcriptional activator of human estrogen receptor  $\alpha$  [ER $\alpha$ ] and ER $\beta$  in cell culture. A BPA metabolite, 4-methyl-2,4-bis(4-hydroxyphenyl)pent-1-ene [MBP], has transcriptional activity at nM concentrations, which is 1000-fold lower than the concentration for estrogenic activity of BPA, suggesting that MBP may be an environmental estrogen. To investigate the structural basis for the activity of MBP at nM concentrations and the lower activity of BPA for human ER $\alpha$  and ER $\beta$ , we constructed 3D models of human ER $\alpha$  and ER $\beta$  with MBP and BPA for comparison with estradiol in these ERs. These 3D models suggest that MBP, but not BPA, has key contacts with amino acids in human ER $\alpha$  and ER $\beta$  that are important in binding of estradiol by these receptors. Metabolism of BPA to MBP increases the spacing between two phenolic rings, resulting in contacts between MBP and ER $\alpha$  and ER $\beta$  that mimic those of estradiol with these ERs. Mutagenesis of residues on these ERs that contact the phenolic hydroxyls will provide a test for our 3D models. Other environmental chemicals containing two appropriately spaced phenolic rings and an aliphatic spacer instead of an estrogenic B and C ring also may bind to ER $\alpha$  or ER $\beta$  and interfere with normal estrogen physiology. This analysis also may be useful in designing novel chemicals for regulating the actions of human ER $\alpha$  and ER $\beta$ .

**Citation:** Baker ME, Chandsawangbhuwana C (2012) 3D Models of MBP, a Biologically Active Metabolite of Bisphenol A, in Human Estrogen Receptor  $\alpha$  and Estrogen Receptor  $\beta$ . PLoS ONE 7(10): e46078. doi:10.1371/journal.pone.0046078

**Editor:** Vincent Laudet, Ecole Normale Supérieure de Lyon, France

**Received:** April 12, 2012; **Accepted:** August 29, 2012; **Published:** October 4, 2012

**Copyright:** © 2012 Baker, Chandsawangbhuwana. This is an open-access article distributed under the terms of the Creative Commons Attribution License, which permits unrestricted use, distribution, and reproduction in any medium, provided the original author and source are credited.

**Funding:** The authors have no support or funding to report.

**Competing Interests:** The authors have declared that no competing interests exist.

\* E-mail: mbaker@ucsd.edu

## Introduction

One consequence of our industrial society is the presence of novel environmental chemicals that disrupt normal physiological responses in humans, other vertebrates, as well as invertebrates [1,2]. Many of these chemicals are small hydrophobic molecules that resemble steroids, thyroid hormone, retinoids and other lipophilic hormones and, as a result bind to their receptors in vertebrates [3,4,5,6,7]. Some of these chemicals act like hormones, while others act like anti-hormones. In either case, they disrupt normal endocrine physiology.

An endocrine disruptor of much concern is bisphenol A [BPA] because it is widely dispersed in the environment due to the presence of BPA in polycarbonate plastics, which are used in containers for food and water, including baby bottles, as well as the linings of metal cans used for food and beverages [8,9,10]. Leaching of the BPA monomer from these sources into food, milk and the environment exposes humans [11,12,13] and wildlife [2,14] to BPA.

A consequence of the widespread use of BPA is that over 90% of the general population is exposed to BPA [9,13,15]. BPA levels range from 0.3 nM to 40 nM in maternal plasma and fetal human serum [8,10,11]. Moreover, due to the lipophilic nature of BPA, it can accumulate in fat [16].

BPA has some structural similarity to estradiol and diethylstilbestrol [Figure 1], and, indeed, BPA binds to human estrogen receptor  $\alpha$  [ER $\alpha$ ] and ER $\beta$  and is a transcriptional activator of these ERs [17,18,19,20]. However, BPA's binding affinity and transcriptional activity for these ERs is over 1000-fold lower than that of E2 [17,18,19,20], which makes it unlikely that nM concentrations of BPA would disrupt estrogen physiology. Nevertheless, *in vivo* studies indicate that BPA is active at 1 nM to 10 nM [8,10,15,21], which raises the possibility that BPA is metabolized to a more active endocrine disruptor. One such candidate metabolite is 4-methyl-2,4-bis(4-hydroxyphenyl)pent-1-ene [MBP] [Figure 1], which has about 1000-fold higher estrogenic activity than BPA [22,23]. To begin to understand the structural basis for the high estrogenic activity of MBP and its higher affinity compared to BPA for human ER $\alpha$  and ER $\beta$ , we constructed 3D models of MBP and BPA in human ER $\alpha$  and ER $\beta$ . We find that MBP retains key contacts with human ER $\alpha$  and ER $\beta$  that are important in activation of these receptors by estradiol. We also find that one phenolic ring of BPA can mimic binding of the A ring of E2 to ER $\alpha$  and ER $\beta$ , which would account for the binding of BPA to these ERs. However, the second phenolic ring on BPA lacks some key contacts that are found between E2 and both ERs, which may explain the lower estrogenic activity of BPA. In addition to elucidating the

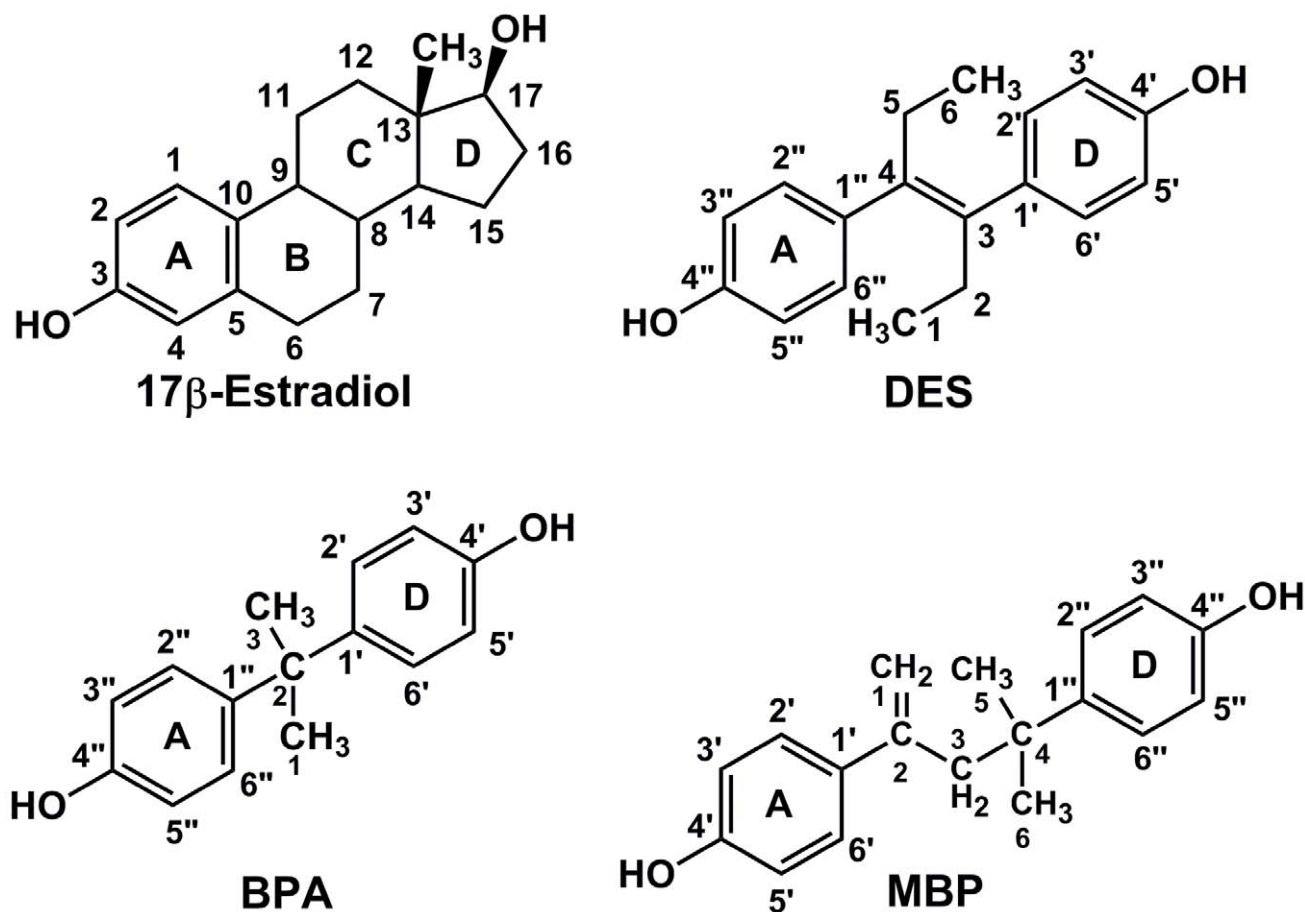


**Figure 1. Structures of MBP, BPA, E2 and DES.** MBP, BPA and DES have a phenolic ring that can mimic the A ring on E2 in binding to ER $\alpha$  and ER $\beta$ . The spacing between the first and second phenolic hydroxyls on MBP and DES is similar to that between C3 hydroxyl and the 17 $\beta$ -hydroxyl on E2. In contrast, the distance between the two phenolic hydroxyls in BPA is shorter than that in E2. doi:10.1371/journal.pone.0046078.g001

interaction of MBP and BPA with both human ERs, this analysis may be useful in designing novel chemicals for regulating the actions of human ER $\alpha$  and ER $\beta$ .

## Methods

Human ER $\alpha$  [24] was downloaded from the Protein Data Bank [PDB] as a template for docking of MBP and BPA. ChemDraw 3D was used to create PDB files for MBP and BPA, which were docked to human ER $\alpha$  [PDB:1G50] with AutoDock 4 [25,26] and AutoDock Vina [27]. The grid was centered over the estrogen binding site in human ER $\alpha$ . AutoDock 4 was run using the Lamarckian Genetic Algorithm for 250 trials of 5 million energy evaluations. AutoDock Vina was run with a setting of 20 for exhaustiveness and poses for the 100 lowest energies were collected.

The crystal structure of ER $\beta$  complexed with E2 [PDB:3OLS] [28] was selected for docking MBP and BPA. As was found in other ER $\beta$  structures in the PDB, 3OLS lacks coordinates for five amino acids corresponding to residues 416–420. To model the missing amino acids, we used the Homology option in Insight II and the 1G50 structure for human ER $\alpha$  as a template. A PDB file of the complete ER $\beta$  with E2 was refined with Discover 3 with the CVFF force field and a distant

dependent dielectric constant of 2 for 50 iterations. We docked MBP and BPA into this PDB file of human ER $\beta$  with AutoDock 4 and AutoDockVina [27] with the settings used previously for human ER $\alpha$ .

The lowest energy complexes of MBP and BPA in ER $\alpha$  and ER $\beta$ , as calculated by AutoDock 4 and AutoDock Vina, were refined with the Discover 3 software in Insight II. For this energy minimization step, Discover 3 was used with the CVFF force field and a distant dependent dielectric constant of 2 for 10,000 iterations. During this refinement step, both the amino acids on the ERs and MBP and BPA rearrange their positions so as to lower the Gibbs free energy of the complex.

## Docking Energy Analysis

We used X-Score [29,30] and DSX [DrugScore eXtended] [31] to estimate the relative binding energy of MBP and BPA in the various configurations in ER $\alpha$  and ER $\beta$ . X-Score uses an empirical scoring function to estimate the affinity of a ligand for a protein. DSX uses a knowledge-based scoring function based on the DrugScore formalism [32] to estimate the affinity of a ligand for a protein. In comparing the score of two ligands for a protein, the ligand with the larger negative score has the higher affinity.

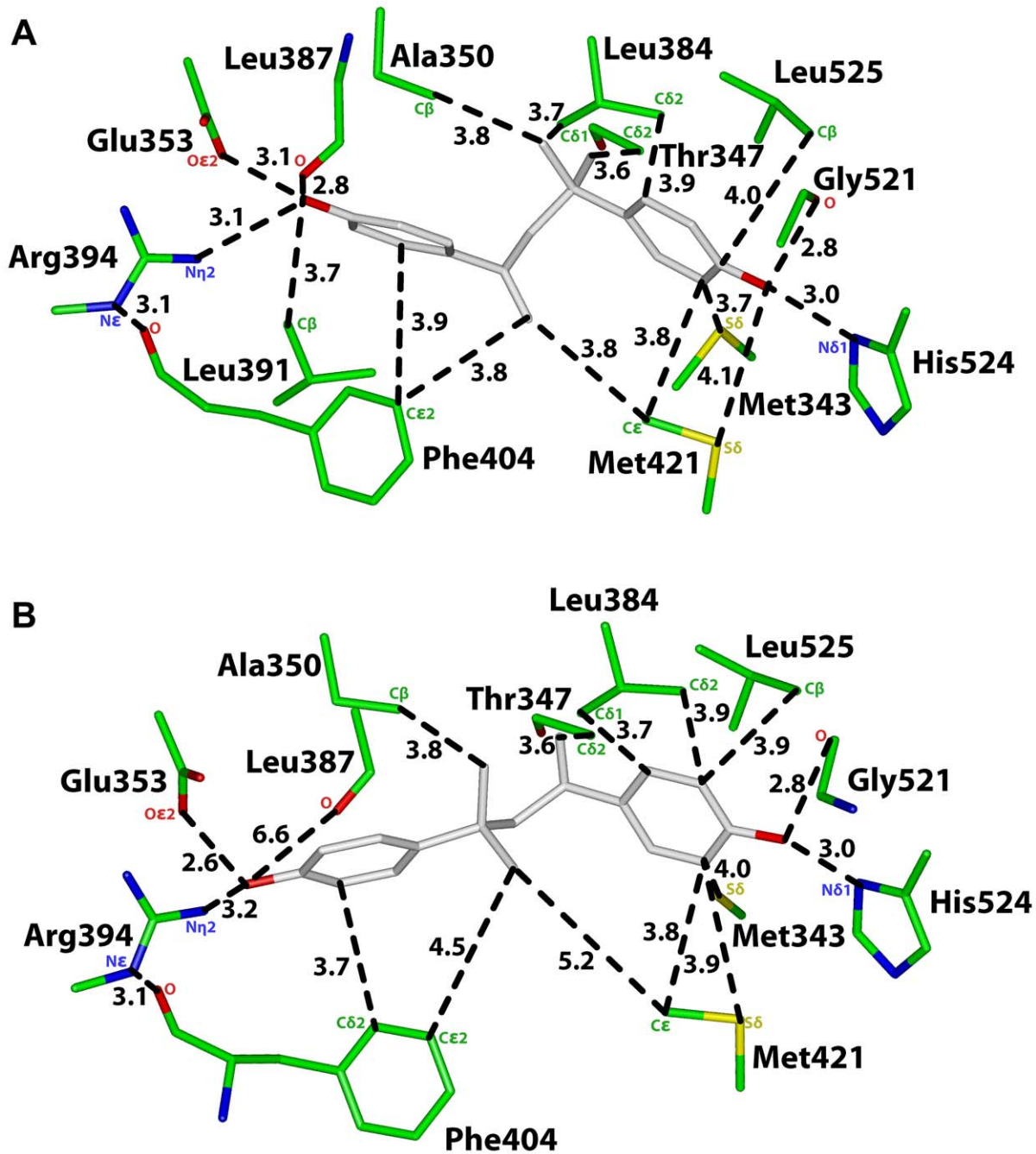


**Figure 2. Analysis of two 3D models of MBP in human ER $\alpha$ .** **A.** 3D model of MBP in orientation 1 in human ER $\alpha$ . The first phenolic ring on MBP contacts Glu-353, Arg-394 and Phe-404 on ER $\alpha$  and the second phenolic ring contacts Gly-521, His-524 and Leu-525. Favorable van der Waals contacts have a distance of 4.25 Å or less between MBP and amino acids on ER $\alpha$ . **B.** 3D model of MBP in orientation 2 in human ER $\alpha$ . The first phenolic ring on MBP contacts Glu-353, Arg-394 and Phe-404 on ER $\alpha$ , and the second phenolic ring contacts Gly-521, His-524 and Leu-525. However, in contrast to Orientation 1, the backbone oxygen on Leu-387 does not contact the phenolic hydroxyl on MBP. Phe-404 and Met-421 do not have van der Waals contacts with the linker between the two phenolic rings on MBP. doi:10.1371/journal.pone.0046078.g002

## Results

### Docking of MBP and BPA to Human ER $\alpha$ and ER $\beta$

Docking of MBP into human ER $\alpha$  and ER $\beta$  using AutoDock 4 [25,26] and AutoDock Vina [27] gave two symmetric poses, which is not surprising because MBP has a phenolic ring at each end

[Figure 1]. BPA also had two poses for one of the rings in ER $\alpha$  and ER $\beta$ . We analyzed both poses for MBP and BPA in human ER $\alpha$  and ER $\beta$ . In our analysis of the 3D models of MBP and BPA in both ERs, we use the term “first phenolic ring” to describe the ring that has contacts with ER $\alpha$  and ER $\beta$  that are similar to the A ring of E2.

**Table 1.** Distances between MBP and ER $\alpha$ .

Figure 2A	ER $\alpha$	MBP	Distance
Orientation 1	O $\epsilon$ 2, Glu-353	O4'	3.1 Å
	N $\eta$ 2, Arg-394	O4'	3.1 Å
	O, Leu-387	O4'	2.8 Å
	C $\beta$ , Leu-391	O4'	3.7 Å
	C $\epsilon$ 2, Phe-404	C2'	3.9 Å
	C $\epsilon$ 2, Phe-404	C1	3.8 Å
	N $\delta$ 1, His-524	O4''	3.0 Å
	O, Gly-521	O4''	2.8 Å
	C $\beta$ , Leu-525	C4''	4.0 Å
	S $\delta$ , Met-343	C3''	3.7 Å
	S $\delta$ , Met-421	O4''	4.1 Å
	C $\epsilon$ , Met-421	C3''	3.8 Å
	C $\delta$ 2, Leu384	C6	3.9 Å
	C $\delta$ 1, Leu384	C6	3.7 Å
	C $\delta$ 2, Thr-347	C5	3.6 Å
C $\beta$ , Ala-350	C6	3.8 Å	
Figure 2B	ER $\alpha$	MBP	Distance
Orientation 2	O $\epsilon$ 2, Glu-353	O4''	2.6 Å
	N $\eta$ 2, Arg-394	O4''	3.2 Å
	O, Leu-387	O4''	6.6 Å
	C $\beta$ , Leu-391	O4''	3.7 Å
	C $\delta$ 2, Phe-404	C3''	3.9 Å
	C $\epsilon$ 2, Phe-404	C6	4.5 Å
	N $\delta$ 1, His-524	O4'	3.0 Å
	O, Gly-521	O4'	2.8 Å
	C $\beta$ , Leu-525	C3'	3.9 Å
	S $\delta$ , Met-343	C5'	4.0 Å
	S $\delta$ , Met-421	C5'	3.9 Å
	C $\epsilon$ , Met-421	C5'	3.9 Å
	C $\epsilon$ , Met-421	C6	5.2 Å
	C $\delta$ 1, Leu384	C2'	3.7 Å
	C $\delta$ 2, Leu384	C3'	3.9 Å
C $\delta$ 2, Thr-347	C1	3.6 Å	
C $\beta$ , Ala-350	C5	3.8 Å	

doi:10.1371/journal.pone.0046078.t001

Analysis of the crystal structures of ER $\alpha$  complexed with E2 [33,34] and other estrogens [35] revealed that Glu-353 and Arg394 have important stabilizing contacts with the C3 hydroxyl on the A ring and His-524 with the 17 $\beta$ -hydroxyl on the D ring. Glu-305, Arg-346 and His-475 on ER $\beta$  have similar stabilizing contacts with estrogens. As reported below, the presence or absence of these contacts in the 3D models of ER $\alpha$  and ER $\beta$  with BPA and MBP is important analyzing the interaction between these chemicals and the ERs.

#### Analysis of MBP in Orientation 1 in Human ER $\alpha$

In Figure 2A, we show the 3D model of MBP in human ER $\alpha$  in Orientation 1, in which C1 on MBP is closest to first phenolic

ring. The distances between MBP and ER $\alpha$  are shown in Figure 2A and Table 1. For comparison, in Figure 3A and Table 2 we show the distances between E2 and human ER $\alpha$  [33,35,36,37,38].

The first phenolic ring on MBP has contacts that are similar to that of the A ring on E2 with human ER $\alpha$  [33,34,39]. The phenolic hydroxyl on MBP is 3.1 Å from O $\epsilon$ 2 on Glu-353, 3.1 Å from N $\eta$ 2 on Arg-394 and 2.8 Å from the backbone oxygen of Leu-387. MBP is 3.9 Å from C $\epsilon$ 2 on Phe-404 [Figure 2A, Table 1]. These contacts are similar to that for E2 with human ER $\alpha$ , except that C $\delta$ 2 on Leu-387 does not contact the phenolic hydroxyl on MBP, in contrast to the contact between Leu-387 and E2 in human ER $\alpha$  [Figure 3A, Table 2].

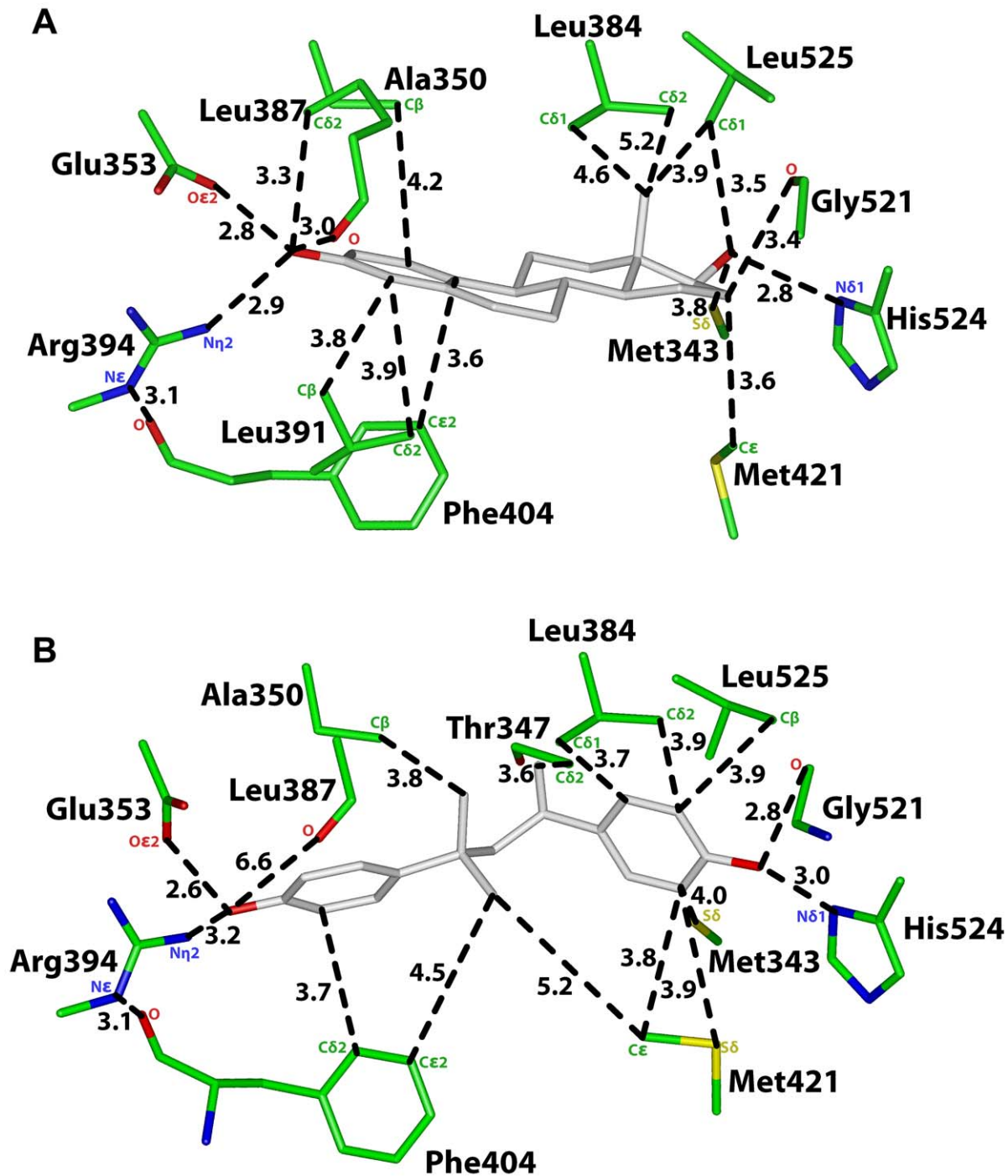


**Figure 3. Interaction of E2 with amino acids in human ER $\alpha$  and ER $\beta$ .** **A.** Interaction of E2 with human ER $\alpha$  [24,33,34,36,37,38,39]. The phenolic hydroxyl of E2 contacts Glu-353, Arg-394 and Leu-387. The 17 $\beta$ -hydroxyl contacts His524 and Leu-525. The D ring contacts Met343, Met421, Gly-521 and Ile-424. Favorable van der Waals contacts have a distance of 4.25 Å or less between E2 and amino acids on ER $\alpha$ . **B.** Interaction of E2 with human ER $\beta$  [28]. The phenolic hydroxyl of E2 contacts Glu-305, Arg-346 and Leu-339. The 17 $\beta$ -hydroxyl contacts Gly-472, His473 and Leu-476. The D ring contacts Met-336 and Ile-373. Favorable van der Waals contacts have a distance of 4.25 Å or less between E2 and amino acids on ER $\beta$ . doi:10.1371/journal.pone.0046078.g003

The second phenolic hydroxyl in MBP is 3 Å, 2.8 Å and 4 Å from N $\delta$ 1 on His-524, the backbone oxygen on Gly-521 and C $\beta$  on Leu-525, respectively, on ER $\alpha$  [Figure 2A]. This phenolic hydroxyl also contacts Met-343 and Met-421 on ER $\alpha$ . These

five residues stabilize the D ring on E2 in human ER $\alpha$  [Figure 3A].

There are, however, differences in some interactions between ER $\alpha$  and MBP compared to that with E2. While Gly-521 and

**Table 2.** Distances between E2 and ER $\alpha$  and ER $\beta$ .

<b>Figure 3A</b>	<b>ER<math>\alpha</math></b>	<b>E2</b>	<b>Distance</b>
Crystal Structure	O $\epsilon$ 2, Glu-353	O3	2.8 Å
PDB: 1G50	N $\eta$ 2, Arg-394	O3	2.9 Å
	O, Leu-387	O3	3.0 Å
	C $\delta$ 2, Leu-387	O3	3.0 Å
	C $\epsilon$ 2, Phe-404	C10	3.6 Å
	N $\delta$ 1, His-524	O17	2.8 Å
	O, Gly-521	O17	
	O, Gly-521	C16	3.4 Å
	C $\delta$ 1 Leu-525	O17	3.5 Å
	C $\delta$ 1 Leu-525	C18	3.9 Å
	S $\delta$ , Met-343	O17	3.8 Å
	C $\epsilon$ , Met-421	O16	3.6 Å
	S $\delta$ , Met-421	O17	
	C $\delta$ 2, Leu384	C18	5.2 Å
	C $\delta$ 1, Leu384	C18	4.6 Å
	C $\beta$ , Ala-350	C1	4.2 Å
C $\beta$ , Leu-391	C4	3.8 Å	
C $\delta$ 2, Leu-391	C4'	3.9 Å	
<b>Figure 3B</b>	<b>ER<math>\beta</math></b>	<b>E2</b>	<b>Distance</b>
Crystal Structure	O $\epsilon$ 2, Glu-305	O3	2.6 Å
PDB: 3OLS	N $\eta$ 2, Arg-346	O3	3.0 Å
	O, Leu-339	O3	3.4 Å
	C $\beta$ , Leu-339	C2	4.0 Å
	C $\delta$ 1, Leu-343	C4	4.0 Å
	C $\delta$ 2, Leu-343	C4	3.9 Å
	C $\epsilon$ 2, Phe-356	C5	3.7 Å
	C $\beta$ , Ala-302	C1	3.9 Å
	O, Gly-472	O17	3.9 Å
	N $\delta$ 1, His-475	O17	3.0 Å
	C $\beta$ , Leu-476	O17	3.4 Å
	C $\delta$ 2 Leu-476	C18	3.9 Å
	C $\epsilon$ , Met-295	O17	3.5 Å
	S $\delta$ , Met-336	C18	3.7 Å
	C $\epsilon$ 2, Met-336	C18	3.4 Å
	C $\delta$ 1, Ile-373	C16	3.8 Å
	C $\epsilon$ , Met-421	O17	3.5 Å

doi:10.1371/journal.pone.0046078.t002

Met-421 contact the second phenolic hydroxyl on MBP [Figure 2A], Gly-521 and Met-421 contact C16 on E2 in ER $\alpha$  [Figure 3A]. While Leu-384 has two van der Waals contacts with MBP, Leu-384 does not contact E2 in ER $\alpha$ . While Thr-347 has a van der Waals contact with MBP, Thr-347 does not contact E2 in ER $\alpha$ . While C $\beta$  on Leu-391 is 3.7 Å from the first phenolic hydroxyl on MBP, this contact is absent between ER $\alpha$  and E2. While Ala-350 contacts the linker between the two phenolic rings on MBP, Ala-350 contacts C1 on the A ring in E2 in ER $\alpha$ . Phe-404 and Met-421 have van

der Waals contacts with C1 on MBP, which has no equivalent in E2 in ER $\alpha$ .

#### Analysis of MBP in Orientation 2 in Human ER $\alpha$

As shown in Figure 2B and Table 1, analysis of ER $\alpha$  with MBP in Orientation 2 reveals that MBP has contacts with Glu-353, Arg-394, Phe-404, Met-343, Leu-384, Met-421, Gly-521, His-524 and Leu-525 that are similar to those found in Orientation 1 of MBP in ER $\alpha$ . Due to the reversed orientation of MBP in ER $\alpha$ , C1 on MBP has a van der Waals contact with Thr-347, and the other part of the linker contacts Ala-350.

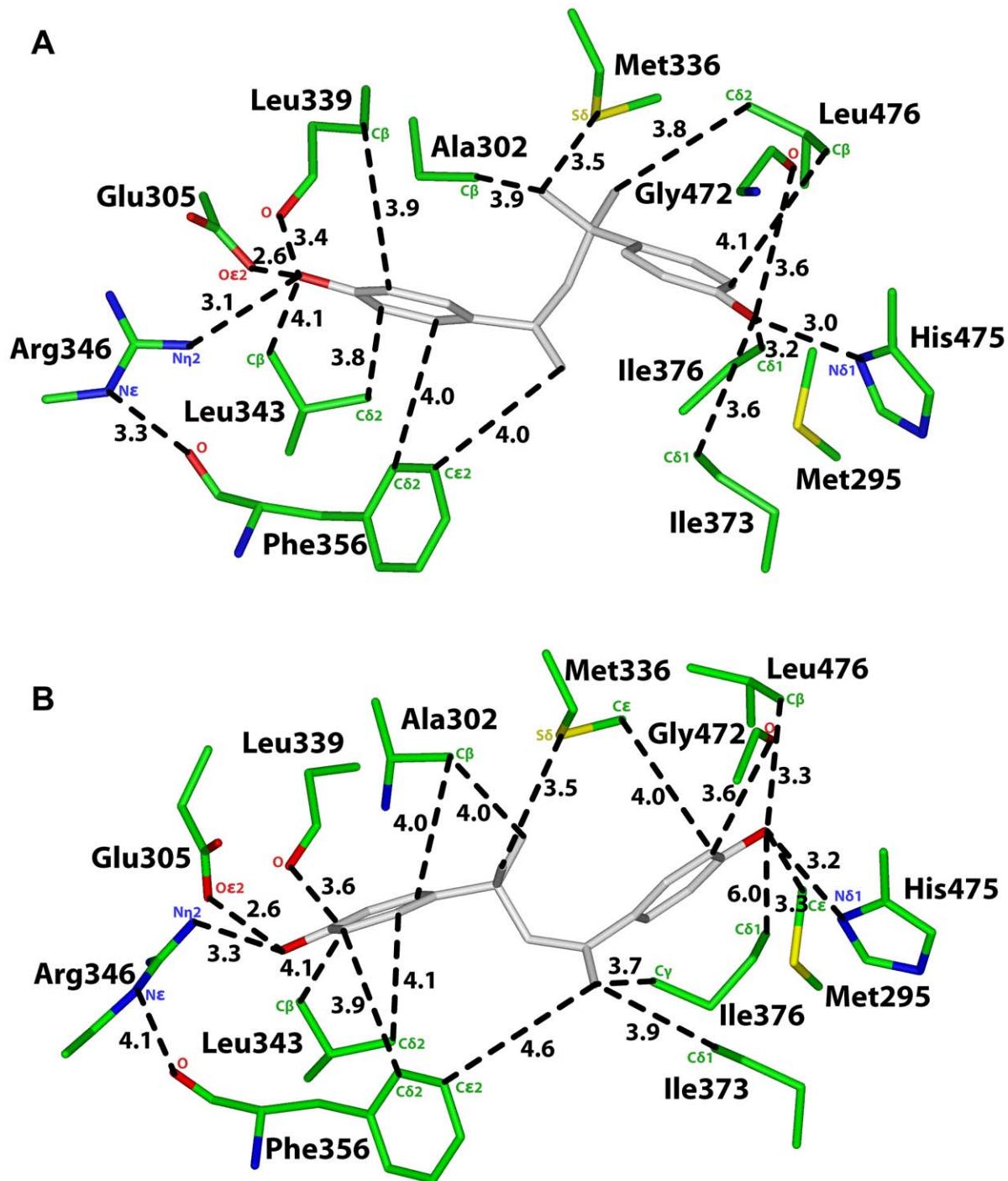


**Figure 4. Analysis of two 3D models of MBP in human ER $\beta$ .** **A.** 3D model of MBP in orientation 1 in human ER $\beta$ . The first phenolic ring on MBP contacts Glu-305, Arg-346, Leu-339, Leu-343 and Phe-356. The second phenolic ring contacts Gly-472, His-475 and Leu-476, which are important in the interaction of the D ring of E2 with ER $\beta$ . **B.** 3D model of MBP in orientation 2 in human ER $\beta$ . The first phenolic ring on MBP contacts the backbone oxygen on Leu-339, C $\beta$  on Ala-302 and Leu-343. These contacts are absent between MBP in Orientation 2 in ER $\alpha$  [Figure 2B].  
doi:10.1371/journal.pone.0046078.g004

#### Analysis of MBP in Orientation 1 in Human ER $\beta$

Figure 4A shows MBP in Orientation 1 in human ER $\beta$ . For comparison, in Figure 3B, we show E2 in human ER $\beta$  [28]. Many of the contacts between MBP and human ER $\beta$  shown in Figure 4A and Table 3 are similar to that between MBP in Orientation 1 and

human ER $\alpha$  [Figure 2A, Table 2] and between E2 and ER $\beta$  [Figure 3B]. Like the A ring in E2, the first phenolic ring on MBP has stabilizing contacts with Glu-305, Arg-346, Phe-356, Leu-339 and Leu-343 in ER $\beta$ . The second phenolic ring contacts His-475, Gly-472, Leu-476, Ile-373 and Ile-376 [Figure 4A, Table 3].

**Table 3.** Distances between MBP and ER $\beta$ .

Figure 4A	ER $\beta$	MBP	Distance
Orientation 1	O $\epsilon$ 2, Glu-305	O4'	2.6 Å
	N $\eta$ 2, Arg-346	O4'	3.1 Å
	O, Leu-339	O4'	3.4 Å
	C $\beta$ , Leu-343	O4'	3.9 Å
	C $\delta$ 2, Phe-356	C2'	4.0 Å
	C $\epsilon$ 2, Phe-356	C1	4.0 Å
	N $\delta$ 1, His-475	O4''	3.0 Å
	O, Gly-472	O4''	3.6 Å
	C $\beta$ , Leu-476	C3''	4.1 Å
	C $\epsilon$ , Met-295	O4''	5.7 Å
	C $\beta$ , Ala-302	C6	3.9 Å
	S $\delta$ , Met-336	C6	3.5 Å
	C $\delta$ 1, Ile-373	O4''	3.6 Å
	C $\delta$ 1, Ile-376	O4''	3.2 Å
Figure 4B	ER $\beta$	MBP	Distance
Orientation 2	O $\epsilon$ 2, Glu-305	O4''	2.6 Å
	N $\eta$ 2, Arg-346	O4''	3.3 Å
	O, Leu-339	C4''	3.6 Å
	C $\beta$ , Leu-343	C5''	4.1 Å
	C $\delta$ 2, Leu-343	C6''	4.1 Å
	C $\delta$ 2, Phe-356	C5''	3.9 Å
	C $\epsilon$ 2, Phe-356	C1	4.6 Å
	N $\delta$ 1, His-475	O4'	3.2 Å
	O, Gly-472	C5'	3.6 Å
	C $\beta$ , Leu-476	O4'	3.3 Å
	C $\epsilon$ , Met-295	O4'	3.3 Å
	C $\beta$ , Ala-302	C5	4.0 Å
	C $\beta$ , Ala-302	C2''	4.0 Å
	S $\delta$ , Met-336	C6	3.5 Å
	C $\epsilon$ , Met-336	C5'	4.0 Å
	C $\delta$ 1, Ile-373	C1	3.9 Å
	C $\gamma$ , Ile-376	C1	3.7 Å
C $\delta$ 1, Ile-376	O4'	6.0 Å	

doi:10.1371/journal.pone.0046078.t003

### Analysis of MBP in Orientation 2 in Human ER $\beta$

Figure 4B shows MBP in Orientation 2 in human ER $\beta$ . Many of the contacts between MBP in Orientation 2 and human ER $\beta$  [Table 3] are similar to that between MBP in Orientation 1 and human ER $\beta$  [Figure 4A, Table 3]] and between E2 and ER $\beta$  [Table 2]. The backbone oxygen on Leu-339, C $\beta$  on Ala-302 and the side chains on Leu-343 contact the first phenolic ring on MBP. These contacts are absent between MBP in Orientation 2 in ER $\alpha$  [Figure 2B, Table 1].

### Analysis of BPA in Orientation 1 in Human ER $\alpha$

Figure 5A shows BPA in Orientation 1 in human ER $\alpha$ . The phenolic ring on BPA, corresponding to the A ring of E2, has stabilizing contacts with O $\epsilon$ 2 on Glu-353, N $\eta$ 2 on Arg-394, C $\delta$ 2

on Phe-404 and C $\beta$  on Ala-350 [Figure 5A, Table 4]. However, the backbone oxygen on Leu-387 is 6.4 Å from the phenolic hydroxyl and Leu-391 does not have a van der Waals contact with the phenolic ring.

The second phenolic ring does not contact either Gly-521, His-524 or Leu-525 [Table 4]. Instead, phenolic ring moves so that it contacts C $\epsilon$ 2 and C $\eta$  on Phe-404, C $\epsilon$  on Met-421 and C $\delta$ 2 on Ile-424. Also, Ala-350 and Leu-384 and Thr-347 contact the linker on BPA.

### Analysis of BPA in Orientation 2 in Human ER $\alpha$

In Figure 5B, we show BPA in Orientation 2 in human ER $\alpha$ . The first phenolic ring on BPA contacts O $\epsilon$ 2 on Glu-353, N $\eta$ 2 on Arg-394, C $\delta$ 2 on Phe-404 and C $\beta$  on Ala-350 [Figure 5B,

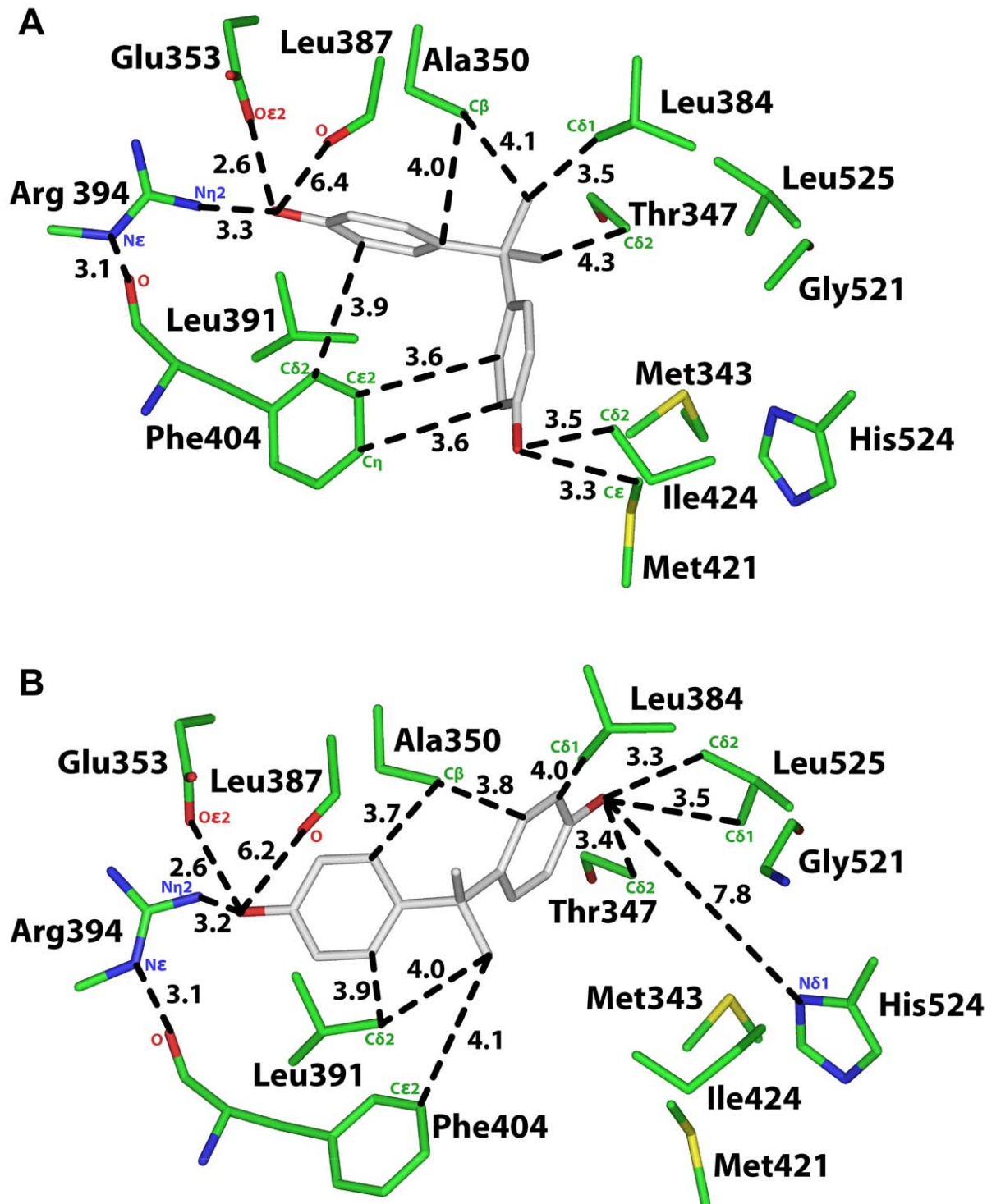


**Figure 5. Analysis of two 3D models of BPA in human ER $\alpha$ .** **A.** 3D model of BPA in orientation 1 in human ER $\alpha$ . The first phenolic ring on BPA contacts Glu-353, Arg-394 and Phe-404 on ER $\alpha$ , but does not contact either Leu-387 or Leu-391. Moreover, the second phenolic ring does not contact either Gly-521, His-524 or Leu-525. Instead, the second phenolic ring contacts Phe-404, Met-421 and Ile-424. **B.** 3D model of BPA in orientation 2 in human ER $\alpha$ . The first phenolic ring on BPA contacts Glu-353 and Arg-394 on ER $\alpha$ , but does not contact Leu-387 or Phe-404. The second phenolic ring does not contact either Gly-521 or His-524. Instead, the second phenolic ring has novel contacts with Thr-347 and Leu-384.  
doi:10.1371/journal.pone.0046078.g005

**Table 4.** Distances between BPA and ER $\alpha$ .

Figure 5A	ER $\alpha$	BPA	Distance
Orientation 1	O $\epsilon$ 2, Glu-353	O4'	2.6 Å
	N $\eta$ 2, Arg-394	O4'	3.3 Å
	O, Leu-387	O4'	6.4 Å
	C $\delta$ 2, Phe-404	C3'	3.9 Å
	C $\epsilon$ 2, Phe-404	C6''	3.6 Å
	C $\eta$ , Phe-404	C5''	3.6 Å
	N $\delta$ 1, His-524	O4''	6.8 Å
	C $\delta$ 1, Leu-384	C1	3.5 Å
	C $\beta$ , Ala-350	C1	4.1 Å
	C $\beta$ , Ala-350	C1'	4.0 Å
	C $\epsilon$ , Met-421	O4''	3.3 Å
	C $\delta$ 2, Ile-424	O4''	3.5 Å
	C $\delta$ 2, Thr-347	C3	4.3 Å
	Figure 5B	ER $\alpha$	BPA
Orientation 2	O $\epsilon$ 2, Glu-353	O4'	2.6 Å
	N $\eta$ 2, Arg-394	O4'	3.2 Å
	O, Leu-387	O4'	6.2 Å
	C $\delta$ 2 Leu-391	C6'	3.9 Å
	C $\delta$ 2 Leu-391	C3	4.0 Å
	C $\epsilon$ 2, Phe-404	C3	4.1 Å
	N $\delta$ 1, His-524	O4''	7.8 Å
	O, Gly-521	O4''	7.4 Å
	C $\beta$ , Leu-525	O4''	3.3 Å
	C $\delta$ 1, Leu-525	O4''	3.5 Å
	S $\delta$ , Met-343	C5''	5.7 Å
	S $\delta$ , Met-421	C5''	7.7 Å
	C $\epsilon$ , Met-421	C5''	7.6 Å
	C $\epsilon$ , Met-421	C6''	7.1 Å
	C $\delta$ 1, Leu384	C3''	4.0 Å
	C $\delta$ 2, Thr-347	O4''	3.4 Å
	C $\beta$ , Ala-350	C2''	3.8 Å
	C $\beta$ , Ala-350	C2'	3.7 Å

doi:10.1371/journal.pone.0046078.t004

Table 4]. Leu-391 has a van der Waals contact with the phenolic ring. However, the backbone oxygen on Leu-387 does not contact BPA.

The second phenolic ring on BPA does not contact either Gly-521, His-524, Met-421 or Ile-424 [Table 4]. Instead, the phenolic hydroxyl contacts Leu-525 and Thr-347. Leu-384 and Ala-350 also contact the second phenolic ring.

#### Analysis of BPA in Orientation 1 in Human ER $\beta$

In Figure 6A, we show BPA in Orientation 1 in human ER $\beta$ . The first phenolic ring on BPA contacts O $\epsilon$ 2 on Glu-305, N $\eta$ 2 on Arg-346, C $\epsilon$ 2 on Phe-404, C $\beta$  on Leu339 and the backbone nitrogen on Ala-302 [Figure 6A, Table 5]. The backbone oxygen on Leu-339 does not contact the phenolic hydroxyl. C $\beta$  on Ala-302 and C $\delta$ 2 on Leu-343 do not contact the phenolic ring.

The second phenolic ring contacts Gly-472, His-475, Leu-476, Ile-373 and Met-336, but the second phenolic ring does not contact Met-295.

#### Analysis of BPA in Orientation 2 in Human ER $\beta$

In Figure 6B, we show the minimized structure of BPA in Orientation 2 in human ER $\beta$ . The first phenolic ring on BPA contacts O $\epsilon$ 2 on Glu-305, N $\eta$ 2 on Arg-346, C $\epsilon$ 2 on Phe-404, C $\beta$  on Ala-350, C $\delta$ 2 on Leu-343 and the backbone oxygen on Leu-339 [Figure 6B, Table 5].

The second phenolic ring does not contact either Gly-472, His-475, Leu-476 or Met-295 [Table 5]. Instead, the phenolic hydroxyl contacts Phe-377 and Ile-373. Interestingly, Phe-356 contacts the second phenolic ring and Met-336 contacts the linker on BPA.

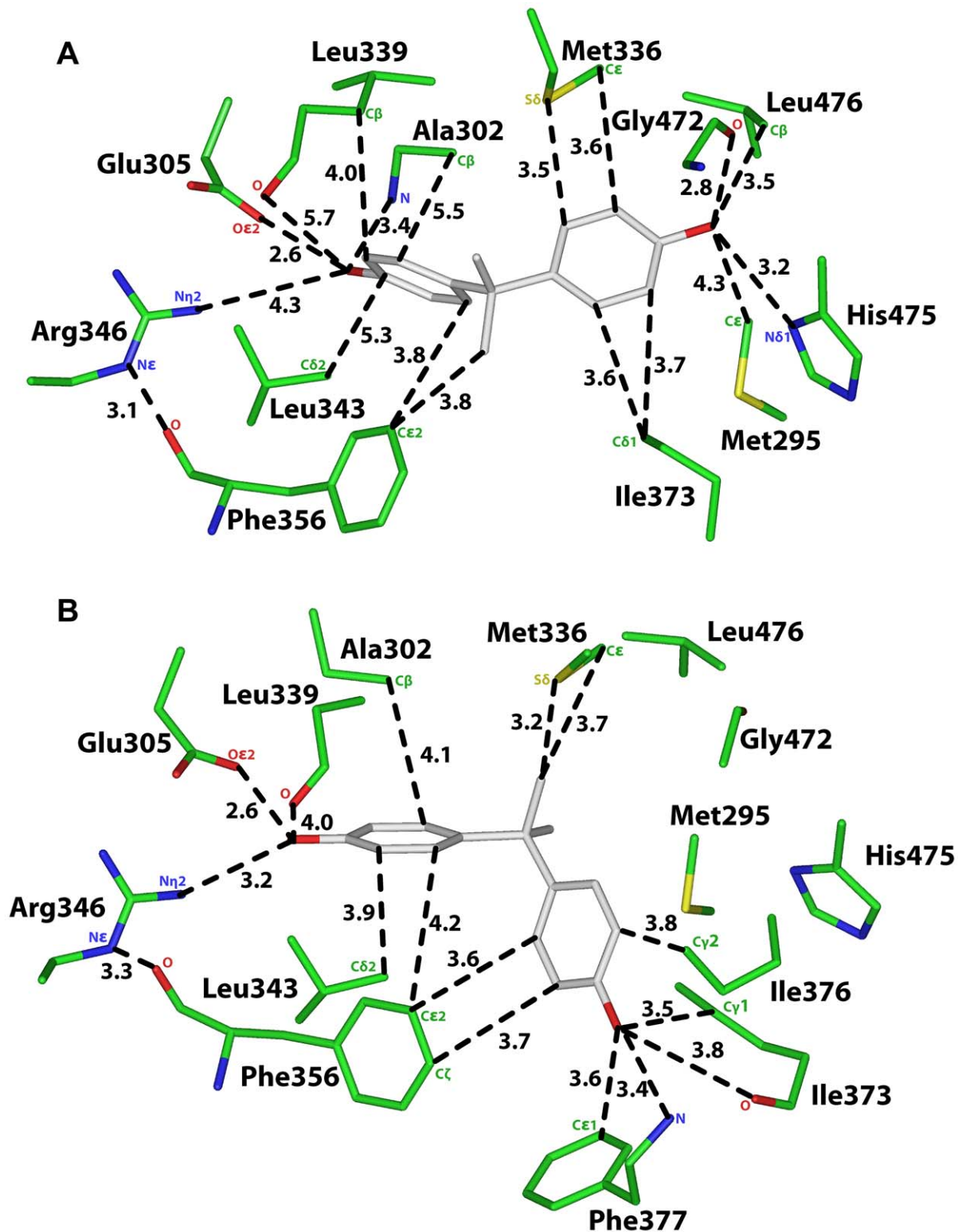


**Figure 6. Analysis of two 3D models of BPA in human ER $\beta$ .** **A.** 3D model of BPA in orientation 1 in human ER $\beta$ . The first phenolic ring on BPA contacts Glu-305, Arg-346, and Phe-356, but does not contact either the backbone oxygen on Leu-339 or C $\delta$ 2 on Leu-343. The second phenolic ring contacts Gly-472, His-475 and Leu-476. **B.** 3D model of BPA in orientation 2 in human ER $\beta$ . The first phenolic ring on BPA contacts Glu-305, Arg-346, Phe-356, the backbone oxygen on Leu-339 and C $\delta$ 2 on Leu-343. The second phenolic ring does not contact either Gly-472, His-475 or Leu-476. doi:10.1371/journal.pone.0046078.g006

**Table 5.** Distances between BPA and ER $\beta$ .

<b>Figure 6A</b>	<b>ER<math>\beta</math></b>	<b>BPA</b>	<b>Distance</b>
Orientation 1	O $\epsilon$ 2, Glu-305	O4'	2.6 Å
	N $\eta$ 2, Arg-346	O4'	4.3 Å
	O, Leu-339	O4'	5.7 Å
	C $\beta$ , Leu-339	O4'	4.0 Å
	C $\delta$ 2, Leu-343	C4'	5.3 Å
	C $\delta$ 2, Phe-356	C3'	4.0 Å
	C $\epsilon$ 2, Phe-356	C2'	3.8 Å
	C $\epsilon$ 2, Phe-356	C3	3.8 Å
	N $\delta$ 1, His-475	O4''	3.2 Å
	O, Gly-472	O4''	2.8 Å
	C $\beta$ , Leu-476	O4''	3.5 Å
	C $\epsilon$ , Met-295	O4''	4.3 Å
	C $\beta$ , Ala-302	C6'	5.5 Å
	N, Ala-302	O4'	3.4 Å
	S $\delta$ , Met-336	C2''	3.5 Å
	C $\epsilon$ , Met-336	C3''	3.6 Å
C $\delta$ 1, Ile-373	C5''	3.7 Å	
C $\delta$ 1, Ile-376	C6''	3.6 Å	
<b>Figure 6B</b>	<b>ER<math>\beta</math></b>	<b>BPA</b>	<b>Distance</b>
Orientation 2	O $\epsilon$ 2, Glu-305	O4'	2.6 Å
	N $\eta$ 2, Arg-346	O4'	3.2 Å
	O, Leu-339	C4'	4.0 Å
	C $\delta$ 2, Leu-343	C5'	3.9 Å
	C $\epsilon$ 2, Phe-356	C6'	4.2 Å
	C $\epsilon$ 2, Phe-356	C6''	3.6 Å
	C $\zeta$ 2, Phe-356	C5''	3.7 Å
	N $\delta$ 1, His-475	O4''	7.1 Å
	O, Gly-472	O4''	8.4 Å
	C $\beta$ , Leu-476	O4''	10.2 Å
	C $\epsilon$ , Met-295	O4''	8.5 Å
	C $\beta$ , Ala-302	C2'	4.1 Å
	S $\delta$ , Met-336	C3	3.2 Å
	C $\epsilon$ , Met-336	C3	3.7 Å
	C $\delta$ 1, Ile-373	C1	3.9 Å
	C $\gamma$ 1, Ile-376	O4''	3.5 Å
	O, Ile-376	O4''	3.8 Å
	C $\epsilon$ 1, Phe-377	O4''	3.6 Å
N, Phe-377	O4''	3.4 Å	

doi:10.1371/journal.pone.0046078.t005

### Docking Energy Analysis

We used X-Score [31] and DSX [31] to estimate the affinity of MBP and BPA in their different orientations in ER $\alpha$  and ER $\beta$ . Tables 6 and 7 summarize these analyses for the X-Score and DSX. For both algorithms, MBP has an affinity for ER $\alpha$  and ER $\beta$  that is closer to that of E2 than is BPA for these receptors. This is consistent with previous assays of the activity of MBP and BPA [22,23].

### Discussion

The leaching of BPA monomers from polycarbonate containers and from liners of metal containers for food and beverages has contributed to the widespread exposure of humans to BPA [2,11,12,13,15]. The relatively low affinity of BPA, compared to E2, for human ER $\alpha$  and ER $\beta$  [17,19,20] would, at first glance, make it unlikely that BPA would be a problem as an estrogenic endocrine disruptor at nM concentrations [9,10,11]. However, it is

**Table 6.** Docking analysis of MBP and BPA in ER $\alpha$  and ER $\beta$ .

Receptor	Ligand	Score	Figure
ER $\alpha$	E2	7.4	Figure 3A
ER $\alpha$	MBP Orientation 1	7.2	Figure 2A
ER $\alpha$	MBP Orientation 2	7.2	Figure 2B
ER $\alpha$	BPA Orientation 1	6.5	Figure 4A
ER $\alpha$	BPA Orientation 2	6.5	Figure 4B
ER $\beta$	E2	7.5	Figure 3A
ER $\beta$	MBP Orientation 1	7.1	Figure 5A
ER $\beta$	MBP Orientation 2	7.2	Figure 5B
ER $\beta$	BPA Orientation 1	6.7	Figure 6A
ER $\beta$	BPA Orientation 2	6.7	Figure 6B

X-Score Analysis of MBP and BPA in ER $\alpha$  and ER $\beta$  [29,30].  
doi:10.1371/journal.pone.0046078.t006

clear that nM concentrations of BPA have estrogenic activity [8,21]. The discovery that MBP, a metabolite of BPA, has a nM affinity for human ER $\alpha$  and ER $\beta$ , suggests that metabolism of BPA to MBP could explain some of effects of BPA on estrogen physiology [22,23].

There is a structural basis for considering BPA and MBP as potential ligands for ER $\alpha$  and ER $\beta$  because BPA and MBP have some structural similarities to known synthetic estrogens [Figure 7]. BPA is a bisphenol linked by one carbon atom [Figure 1] as are cyclofenil-type estrogens [Figure 7], some of which have high affinity for ER $\alpha$  and ER $\beta$  [40]. MBP is a bisphenol linked by three carbon atoms [Figure 1] as is benzestrol [Figure 7], which has a high affinity for ER $\alpha$  and ER $\beta$  [39]. Hexestrol, which is linked by two carbon atoms, also has a high affinity for ER $\alpha$  and ER $\beta$  [18,39]. Thus, it is reasonable to be concerned about potential endocrine disruption by synthetic bisphenols. However, as discussed below, our 3D model of BPA in ERs indicates that BPA does not have the contacts with an ER as is found between fluorine-substituted cyclofenil derivatives [40]. Studies with a wide variety of

synthetic bisphenols [39,40] indicate the length of the carbon linker between bisphenols and side chain substituents on the cyclohexane ring on cyclofenils are important in establishing contacts that lead to high affinity binding to the ER. This is consistent with the analysis of our 3D models of BPA and MBP in ER $\alpha$  and ER $\beta$  as discussed below.

### MBP Retains Important Contacts found between E2 and ER $\alpha$ and ER $\beta$

Our 3D models of MBP and BPA in human ER $\alpha$  and ER $\beta$  [Figures 2, 4–6] identify contacts that can explain MBP's high affinity and BPA's low affinity for both estrogen receptors. A key structural difference between BPA and MBP is the longer spacing between the two phenolic rings in MBP [Figure 1]. As a result, both phenolic rings on MBP form stabilizing contacts with ER $\alpha$  and ER $\beta$  that are similar to that between the A and D rings of E2 and human ER $\alpha$  and ER $\beta$  [28,33,34,35,38,39,41]. These 3D models predict that the second phenolic hydroxyl on MBP has a hydrogen bond with His-524 on ER $\alpha$  and His-475 on ER $\beta$ . Our 3D models can be tested by investigating transcriptional activation by MBP of ER $\alpha$  and ER $\beta$  in which His-524 and His-475, respectively, have been mutated.

### BPA Lacks some Contacts found between E2 and ER $\alpha$ and ER $\beta$

Like the A ring on E2, one phenolic ring on BPA has stabilizing contacts with Glu-353, Arg-394 and Phe-404 in ER $\alpha$  [Figure 5]. Interestingly, Phe-404 also contacts the second phenolic ring. However, the second phenolic ring on BPA does not contact either Gly-521 or His-524 on ER $\alpha$ , which is significant because contacts between E2 and Gly-521 and His-524 in ER $\alpha$  are important in binding of E2 [28,33,35,39,41]. Also, Leu-387 does not contact the first phenolic ring of BPA in either Orientation 1 or Orientation 2. The loss of these contacts between BPA and ER $\alpha$  may explain the lower affinity of BPA for ER $\alpha$ .

In the 3D model of BPA in Orientation 1 in ER $\beta$  [Figure 6A], one phenolic ring on BPA has stabilizing contacts with Glu-305, Arg-346 and Phe-356 in ER $\beta$ . Moreover, the second phenolic ring on BPA contacts Gly-472, His-475 and Leu-476 on ER $\beta$ . Thus, some of the key interactions between the ER $\beta$  and the A and D rings on E2 [Figure 3B] are conserved for BPA in Orientation 1 in ER $\beta$ . However, neither Leu-339 nor Leu-343 contacts the first phenolic ring on BPA. The loss of these contacts would be expected to lower affinity of BPA for ER $\beta$ .

Although BPA in Orientation 2 in ER $\beta$  [Figure 6B] has contacts with Glu-305, Arg-346, Phe-356, Leu-339 and Leu-343, BPA does not contact either Gly-472, His-475 or Leu-476 on ER $\beta$ . Instead, the second phenolic ring has novel contacts with Ile-373, Ile-376, Phe-377 and Phe-356.

### Cellular Context Influences Estrogenic Activity of MBP and BPA

The presence of two phenolic rings in MBP and BPA and the flexibility in the estrogen binding site in ER $\alpha$  and ER $\beta$  [7,33,35,42,43,44,45,46] are important factors in the binding of MBP and BPA to these ERs. The equilibrium dissociation constant of BPA for ER $\alpha$  and ER $\beta$  is about 195 nM and 35 nM respectively [18]. Using a different binding assay, IC<sub>50</sub>s [23] for binding of BPA and MBP to ER $\alpha$  and ER $\beta$  were reported. BPA and MBP have IC<sub>50</sub>s of 1.8  $\mu$ M and 52 nM, respectively

**Table 7.** Docking analysis of MBP and BPA in ER $\alpha$  and ER $\beta$ .

Receptor	Ligand	Score	Figure
ER $\alpha$	E2	-116	Figure 3A
ER $\alpha$	MBP Orientation 1	-103	Figure 2A
ER $\alpha$	MBP Orientation 2	-110	Figure 2B
ER $\alpha$	BPA Orientation 1	-84	Figure 4A
ER $\alpha$	BPA Orientation 2	-91	Figure 4B
ER $\beta$	E2	-123	Figure 3B
ER $\beta$	MBP Orientation 1	-112	Figure 5A
ER $\beta$	MBP Orientation 2	-116	Figure 5B
ER $\beta$	BPA Orientation 1	-90	Figure 6A
ER $\beta$	BPA Orientation 2	-89	Figure 6B

DSX Analysis of MBP and BPA in ER $\alpha$  and ER $\beta$  [31,32].  
doi:10.1371/journal.pone.0046078.t007

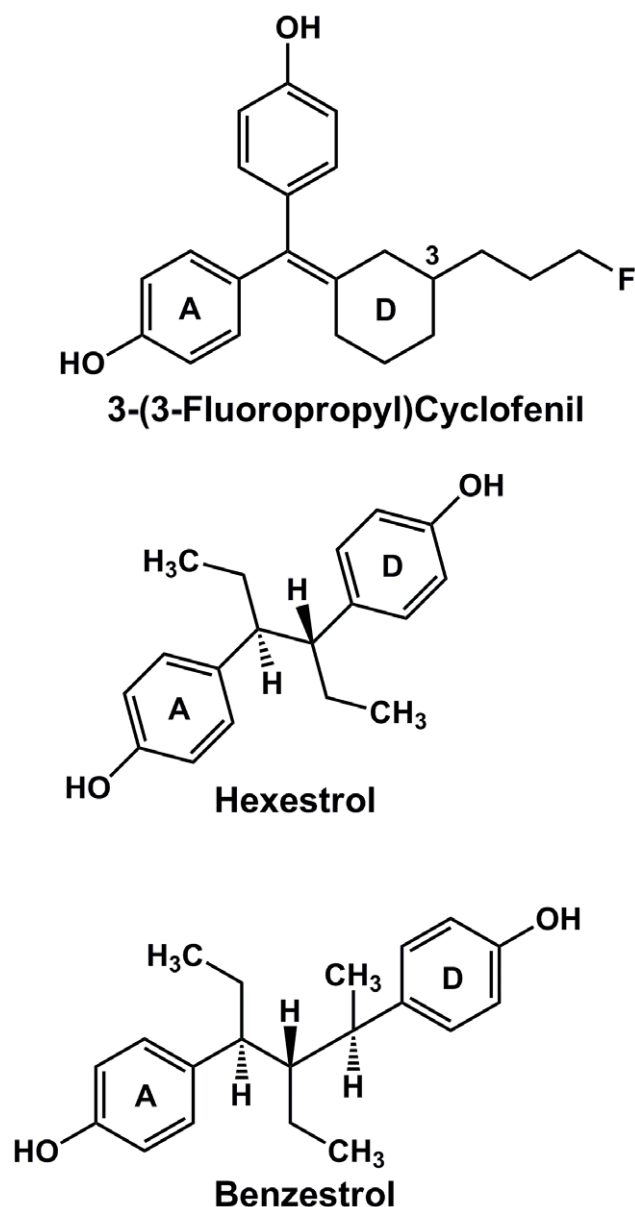


**Figure 7. Structures of bisphenols that are potent synthetic estrogens.** Bisphenols, linked with one, two or three carbons, can have high affinity for ERs. 3-(3-fluoropropyl)cyclofenil, hexestrol and benzeestrol have a higher affinity for ER $\alpha$  that does E2 [18,39,40]. doi:10.1371/journal.pone.0046078.g007

for ER $\alpha$  and IC<sub>50</sub>s of 0.74  $\mu$ M and 0.12  $\mu$ M, respectively, for ER $\beta$ .

## References

- Colborn T, vom Saal FS, Soto AM (1993) Developmental effects of endocrine-disrupting chemicals in wildlife and humans. *Environ Health Perspect* 101: 378–384.
- Diamanti-Kandaraki E, Bourguignon JP, Giudice LC, Hauser R, Prins GS, et al. (2009) Endocrine-disrupting chemicals: an Endocrine Society scientific statement. *Endocr Rev* 30: 293–342.
- Baker ME (2005) Xenobiotics and the evolution of multicellular animals: emergence and diversification of ligand-activated transcription factors. *Integrative and Comparative Biology* 45: 172–178.
- Markov GV, Tavares R, Dauphin-Villemant C, Demeneix BA, Baker ME, et al. (2009) Independent elaboration of steroid hormone signaling pathways in metazoans. *Proc Natl Acad Sci U S A* 106: 11913–11918.
- le Maire A, Bourguet W, Balaguer P (2010) A structural view of nuclear hormone receptor: endocrine disruptor interactions. *Cell Mol Life Sci* 67: 1219–1237.
- Sladek FM (2011) What are nuclear receptor ligands? *Mol Cell Endocrinol* 334: 3–13.
- Baker ME (2011) Insights from the structure of estrogen receptor into the evolution of estrogens: Implications for endocrine disruption. *Biochem Pharmacol* 82: 1–8.
- Welshons WV, Nagel SC, vom Saal FS (2006) Large effects from small exposures. III. Endocrine mechanisms mediating effects of bisphenol A at levels of human exposure. *Endocrinology* 147: S56–69.

Also important for transcriptional activation of ERs and other nuclear receptors by steroids and endocrine disruptors is the binding of co-regulators to the ligand-receptor complex [47,48,49,50,51,52,53]. Thus, even a low affinity ligand such as 27-hydroxy-cholesterol can have transcriptional activity for the ER in the presence of the appropriate co-activator [44].

The interaction of complexes of ER $\alpha$  and ER $\beta$  with different co-regulators may explain the report by Yoshihara et al. [23] that transcriptional activation of ER $\alpha$  and ER $\beta$  by MBP and BPA depended on the cellular context. That is, the estrogenic activity of MBP and BPA is altered in the presence or absence of co-regulators [20,48,50,51,54,55]. In the yeast estrogen screening (YES) assay, the EC<sub>50</sub> potencies for transcriptional activation of ER $\alpha$  by MBP and BPA were 0.7  $\mu$ M and 160  $\mu$ M, respectively. In experiments, which included the Transcriptional Intermediary Factor 2 [TIF2] co-activator in the assay, the EC<sub>50</sub>s for transcriptional activation of rat ER $\alpha$  with TIF2 by MBP and BPA were 8.3 nM and 14  $\mu$ M, respectively, and the EC<sub>50</sub>s for rat ER $\beta$  with TIF2, by MBP and BPA were 8.3 nM and 13  $\mu$ M, respectively. Thus, transcriptional activation of ERs by MBP and BPA in an assay containing TIF2, which mimicked conditions in some mammalian cells, increased by about 10-fold compared to the assay in yeast cells.

Further evidence for the importance of cellular context on transcriptional potency of MBP and BPA comes from experiments using an ERE-luciferase reporter assay in 3T3 cells. Yoshihara et al. [23] found that the EC<sub>50</sub>s for MBP and BPA for ER $\alpha$  were 0.68 nM and 1  $\mu$ M, respectively. For ER $\beta$  in 3T3 cells, the EC<sub>50</sub>s for MBP and BPA were 0.46 nM and 89 nM, respectively. Together these experiments by Yoshihara et al. suggest that MBP is a potential disruptor of physiological responses that are mediated by ER $\alpha$  and ER $\beta$ .

Although MBP and benzeestrol have a three carbon linker between their two phenols, their linkers are different. Despite this difference, nM concentrations of MBP activate transcription of the ER in mammalian cells. This raises the possibility that other environmental chemicals with two phenolic rings connected with novel aliphatic linkers may have a physiologically relevant activity towards ER $\alpha$  and ER $\beta$  in cells with co-activators that can activate the chemical-ER complex. We also note that the 3D models of MBP in ER $\alpha$  and ER $\beta$  may be useful in the development of new chemicals for use as selective ER agonists or antagonists.

## Author Contributions

Conceived and designed the experiments: MEB. Performed the experiments: CC. Analyzed the data: CC MEB. Wrote the paper: MEB.

9. Melzer D, Rice NE, Lewis C, Henley WE, Galloway TS (2010) Association of urinary bisphenol A concentration with heart disease: evidence from NHANES 2003/06. *PLoS One* 5: e8673.
10. Vandenberg LN, Chahoud I, Heindel JJ, Padmanabhan V, Paumgarten FJ, et al. (2010) Urinary, circulating, and tissue biomonitoring studies indicate widespread exposure to bisphenol A. *Environ Health Perspect* 118: 1055–1070.
11. Schonfelder G, Wittfoht W, Hopp H, Talsness CE, Paul M, et al. (2002) Parent bisphenol A accumulation in the human maternal-fetal-placental unit. *Environ Health Perspect* 110: A703–707.
12. Vandenberg LN, Hauser R, Marcus M, Olea N, Welshons WV (2007) Human exposure to bisphenol A (BPA). *Reprod Toxicol* 24: 139–177.
13. Calafat AM, Ye X, Wong LY, Reidy JA, Needham LL (2008) Exposure of the U.S. population to bisphenol A and 4-tertiary-octylphenol: 2003–2004. *Environ Health Perspect* 116: 39–44.
14. Oehlmann J, Schulte-Oehlmann U, Kloas W, Jagnytsh O, Lutz I, et al. (2009) A critical analysis of the biological impacts of plasticizers on wildlife. *Philos Trans R Soc Lond B Biol Sci* 364: 2047–2062.
15. Vandenberg LN, Maffini MV, Sonnenschein C, Rubin BS, Soto AM (2009) Bisphenol-A and the great divide: a review of controversies in the field of endocrine disruption. *Endocr Rev* 30: 75–95.
16. Fernandez MF, Arrebola JP, Taoufik J, Navalon A, Ballesteros O, et al. (2007) Bisphenol-A and chlorinated derivatives in adipose tissue of women. *Reprod Toxicol* 24: 259–264.
17. Krishnan AV, Stathis P, Permuth SF, Tokes L, Feldman D (1993) Bisphenol-A: an estrogenic substance is released from polycarbonate flasks during autoclaving. *Endocrinology* 132: 2279–2286.
18. Kuiper GG, Carlsson B, Grandien K, Enmark E, Haggblad J, et al. (1997) Comparison of the ligand binding specificity and transcript tissue distribution of estrogen receptors alpha and beta. *Endocrinology* 138: 863–870.
19. Kuiper GG, Lemmen JC, Carlsson B, Corton JC, Safe SH, et al. (1998) Interaction of estrogenic chemicals and phytoestrogens with estrogen receptor beta. *Endocrinology* 139: 4252–4263.
20. Gould JC, Leonard LS, Maness SC, Wagner BL, Conner K, et al. (1998) Bisphenol A interacts with the estrogen receptor alpha in a distinct manner from estradiol. *Mol Cell Endocrinol* 142: 203–214.
21. Richter CA, Taylor JA, Ruhlen RL, Welshons WV, Vom Saal FS (2007) Estradiol and Bisphenol A stimulate androgen receptor and estrogen receptor gene expression in fetal mouse prostate mesenchyme cells. *Environ Health Perspect* 115: 902–908.
22. Okuda K, Takiguchi M, Yoshihara S (2010) In vivo estrogenic potential of 4-methyl-2,4-bis(4-hydroxyphenyl)pent-1-ene, an active metabolite of bisphenol A, in uterus of ovariectomized rat. *Toxicol Lett* 197: 7–11.
23. Yoshihara S, Mizutare T, Makishima M, Suzuki N, Fujimoto N, et al. (2004) Potent estrogenic metabolites of bisphenol A and bisphenol B formed by rat liver S9 fraction: their structures and estrogenic potency. *Toxicol Sci* 78: 50–59.
24. Eiler S, Gangloff M, Duclaud S, Moras D, Ruff M (2001) Overexpression, purification, and crystal structure of native ER alpha LBD. *Protein Expr Purif* 22: 165–173.
25. Huey R, Morris GM, Olson AJ, Goodsell DS (2007) A semiempirical free energy force field with charge-based desolvation. *J Comput Chem* 28: 1145–1152.
26. Morris GM, Huey R, Lindstrom W, Sammer MF, Belew RK, et al. (2009) AutoDock4 and AutoDockTools4: Automated docking with selective receptor flexibility. *J Comput Chem*.
27. Trott O, Olson AJ (2010) AutoDock Vina: improving the speed and accuracy of docking with a new scoring function, efficient optimization, and multithreading. *J Comput Chem* 31: 455–461.
28. Mocklinghoff S, Rose R, Carraz M, Visser A, Ottmann C, et al. (2010) Synthesis and crystal structure of a phosphorylated estrogen receptor ligand binding domain. *Chembiochem* 11: 2251–2254.
29. Cheng T, Li X, Li Y, Liu Z, Wang R (2009) Comparative assessment of scoring functions on a diverse test set. *J Chem Inf Model* 49: 1079–1093.
30. Wang R, Lai L, Wang S (2002) Further development and validation of empirical scoring functions for structure-based binding affinity prediction. *J Comput Aided Mol Des* 16: 11–26.
31. Neudert G, Klebe G (2011) DSX: a knowledge-based scoring function for the assessment of protein-ligand complexes. *J Chem Inf Model* 51: 2731–2745.
32. Velec HF, Gohlke H, Klebe G (2005) DrugScore(CSD)-knowledge-based scoring function derived from small molecule crystal data with superior recognition rate of near-native ligand poses and better affinity prediction. *J Med Chem* 48: 6296–6303.
33. Brzozowski AM, Pike AC, Dauter Z, Hubbard RE, Bonn T, et al. (1997) Molecular basis of agonism and antagonism in the oestrogen receptor. *Nature* 389: 753–758.
34. Warnmark A, Treuter E, Gustafsson JA, Hubbard RE, Brzozowski AM, et al. (2002) Interaction of transcriptional intermediary factor 2 nuclear receptor box peptides with the coactivator binding site of estrogen receptor alpha. *J Biol Chem* 277: 21862–21868.
35. Shiau AK, Barstad D, Loria PM, Cheng L, Kushner PJ, et al. (1998) The structural basis of estrogen receptor/coactivator recognition and the antagonism of this interaction by tamoxifen. *Cell* 95: 927–937.
36. Tanenbaum DM, Wang Y, Williams SP, Sigler PB (1998) Crystallographic comparison of the estrogen and progesterone receptor's ligand binding domains. *Proc Natl Acad Sci U S A* 95: 5998–6003.
37. Baker ME, Chang DJ (2009) 3D model of amphioxus steroid receptor complexed with estradiol. *Biochem Biophys Res Commun* 386: 516–520.
38. Baker ME, Chang DJ, Chandsawangbhuwana C (2009) 3D model of lamprey estrogen receptor with estradiol and 15alpha-hydroxy-estradiol. *PLoS One* 4: e6038.
39. Katzenellenbogen JA (2011) The 2010 Philip S. Portoghesi Medicinal Chemistry Lectureship: addressing the "core issue" in the design of estrogen receptor ligands. *J Med Chem* 54: 5271–5282.
40. Seo JW, Comminos JS, Chi DY, Kim DW, Carlson KE, et al. (2006) Fluorine-substituted cyclofenil derivatives as estrogen receptor ligands: synthesis and structure-affinity relationship study of potential positron emission tomography agents for imaging estrogen receptors in breast cancer. *J Med Chem* 49: 2496–2511.
41. Celik L, Lund JD, Schiott B (2007) Conformational dynamics of the estrogen receptor alpha: molecular dynamics simulations of the influence of binding site structure on protein dynamics. *Biochemistry* 46: 1743–1758.
42. Manas ES, Unwalla RJ, Xu ZB, Malamas MS, Miller CP, et al. (2004) Structure-based design of estrogen receptor-beta selective ligands. *J Am Chem Soc* 126: 15106–15119.
43. Nettles KW, Bruning JB, Gil G, O'Neill EE, Nowak J, et al. (2007) Structural plasticity in the oestrogen receptor ligand-binding domain. *EMBO Rep* 8: 563–568.
44. DuSell CD, Umetani M, Shaul PW, Mangelsdorf DJ, McDonnell DP (2008) 27-hydroxycholesterol is an endogenous selective estrogen receptor modulator. *Mol Endocrinol* 22: 65–77.
45. Minutolo F, Macchia M, Katzenellenbogen BS, Katzenellenbogen JA (2011) Estrogen receptor beta ligands: recent advances and biomedical applications. *Med Res Rev* 31: 364–442.
46. Lappano R, Recchia AG, De Francesco EM, Angelone T, Cerra MC, et al. (2011) The cholesterol metabolite 25-hydroxycholesterol activates estrogen receptor alpha-mediated signaling in cancer cells and in cardiomyocytes. *PLoS One* 6: e16631.
47. Heery DM, Kalkhoven E, Hoare S, Parker MG (1997) A signature motif in transcriptional co-activators mediates binding to nuclear receptors. *Nature* 387: 733–736.
48. McKenna NJ, O'Malley BW (2002) Combinatorial control of gene expression by nuclear receptors and coregulators. *Cell* 108: 465–474.
49. Smith CL, O'Malley BW (2004) Coregulator function: a key to understanding tissue specificity of selective receptor modulators. *Endocr Rev* 25: 45–71.
50. Jeyakumar M, Carlson KE, Gunther JR, Katzenellenbogen JA (2011) Exploration of dimensions of estrogen potency: parsing ligand binding and coactivator binding affinities. *J Biol Chem* 286: 12971–12982.
51. Billon-Gales A, Krust A, Fontaine C, Abot A, Flouriot G, et al. (2011) Activation function 2 (AF2) of estrogen receptor-alpha is required for the atheroprotective action of estradiol but not to accelerate endothelial healing. *Proc Natl Acad Sci U S A* 108: 13311–13316.
52. McInerney EM, Rose DW, Flynn SE, Westin S, Mullen TM, et al. (1998) Determinants of coactivator LXXLL motif specificity in nuclear receptor transcriptional activation. *Genes Dev* 12: 3357–3368.
53. Voegel JJ, Heine MJ, Tini M, Vivat V, Chambon P, et al. (1998) The coactivator TIF2 contains three nuclear receptor-binding motifs and mediates transactivation through CBP binding-dependent and -independent pathways. *EMBO J* 17: 507–519.
54. Hall JM, McDonnell DP, Korach KS (2002) Allosteric regulation of estrogen receptor structure, function, and coactivator recruitment by different estrogen response elements. *Mol Endocrinol* 16: 469–486.
55. Hall JM, Korach KS (2002) Analysis of the molecular mechanisms of human estrogen receptors alpha and beta reveals differential specificity in target promoter regulation by xenoestrogens. *J Biol Chem* 277: 44455–44461.